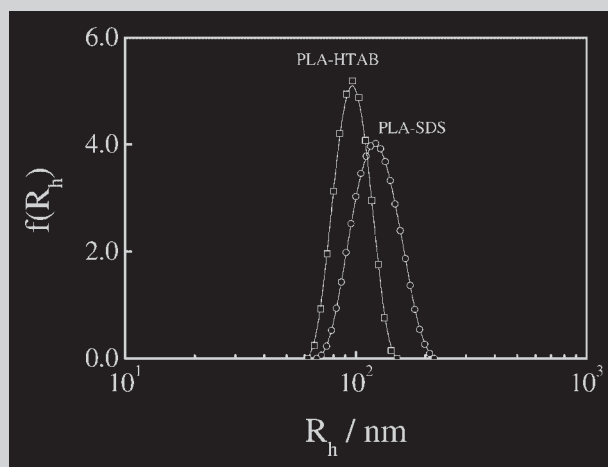


Summary: In the presence of surfactant, water-insoluble poly(D,L-lactide) (PLA) was dispersed into narrowly distributed nanoparticles stable in water via microphase inversion. The structure and degradation of such formed nanoparticles were investigated by a combination of static and dynamic laser light scattering. Our results revealed that the degradation rate increased with the temperature and pH so that the degradation could be regulated from minutes to days. Using anionic sodium dodecyl sulfate (SDS) as stabilizer resulted in a slower degradation than using cationic hexadecyltrimethylammonium bromide (HTAB). The phthalocyanine chromophores (PC) could be encapsulated inside these PLA nanoparticles. The degradation of individual PLA nanoparticles led to a controllable releasing of PC. The absorption and fluorescence studies revealed a correlation between the degradation and the releasing of PC. Our results showed that a higher PC/PLA ratio could lead to a faster degradation.



Hydrodynamic radius distributions $f(R_h)$ of PLA-SDS and PLA-HTAB nanoparticles.

Formation and Degradation of Poly(D,L-lactide) Nanoparticles and Their Potential Application as Controllable Releasing Devices

Yue Zhao,^{*1a} Jie Fu,² Dennis K. P. Ng,³ Chi Wu^{1,3}

¹The Open Laboratory of Bond-selective Chemistry, Department of Chemical Physics, University of Science and Technology of China, Hefei, Anhui, China

E-mail: yzhao@alloy.polym.kyoto-u.ac.jp

²College of Material Science and Engineering, Wuhan University of Technology, Wuhan, Hubei, China

³Department of Chemistry, The Chinese University of Hong Kong, Shatin, N.T., Hong Kong, China

Received: May 26, 2004; Revised: July 22, 2004; Accepted: July 22, 2004; DOI: 10.1002/mabi.200400072

Keywords: controllable releasing; degradation; poly(D,L-lactide)

Introduction

Biocompatible and biodegradable polymers have recently attracted much attention. Besides being environmental friendly, they also have potential biomedical applications, such as surgical sutures, orthopedic implants, scaffolds for cells in tissue engineering, and controllable drug releasing devices.^[1–5] Aliphatic polyesters, such as poly(lactic acid) (PLA), poly(glycolic acid) (PGA) and poly(ϵ -caprolactone) (PCL), are often used because of their biocompatibility and non-toxicity.^[6–9] The biodegradation of these polyesters

often leads to pharmacologically inactive substances, such as lactic acid from PLA and 6-hydroxycaproic acid from PCL, which are absorbable by body or removable by metabolism.^[10,11] Therefore, aliphatic polyesters have a distinct advantage over other types of biomedical materials because it is not necessary to remove them after operation. The biodegradation of aliphatic polyesters in aqueous solution has been extensively studied,^[12] but most of the past studies mainly dealt with bulk materials.

On the other hand, polymeric nanoparticles as colloidal drug carriers have recently also attracted much attention. It has been suggested that by regulating the particle size, one could target different organs. Moreover, polymeric particles can be made in various dosage forms, including intravenous

^a Current address: Department of Polymer Chemistry, Kyoto University, Kyoto 615-8510, Japan.

and oral routes to increase the bio-availability and reduce the associated adverse effects.^[13–15] It has been shown that the irritant at the injection site can be minimized by using smaller particles.^[16] Narrowly distributed stable polymeric nanoparticles with an average diameter less than 200 nm are ideal for intravenous injection because they can easily pass through the blood capillary.^[17] It is known that small polymeric nanoparticles can be prepared via the self-assembly of block copolymers in a selective solvent.^[18–21] However, the synthesis of narrowly distributed block copolymers still remains a tedious work. Therefore, it is natural to extend our study on the micronization of conventional biodegradable and biocompatible polymer materials into nanoparticles as controllable releasing devices.

Numerous types of biodegradable polymers have been investigated, but only a few of them have finally reached the stage of clinical application and become commercially available.^[22–24] Poly(D,L-lactide) (PLA) is one of them. Normally, its degradation in bulk is extremely slow. In this study, we successfully dispersed the water-insoluble PLA into small nanoparticles stable in water with the help of different surfactants via microphase inversion. The structure and degradation of such formed nanoparticles were studied by a combination of static and dynamic laser light scattering. In addition, we used phthalocyanine chromophores (PC) to test their potential application as controllable releasing devices in photodynamic therapy (PDT). The releasing of PC was monitored by both absorption and fluorescence spectroscopies.

Experimental Part

Sample Preparation

Poly(D,L-lactide) ($\bar{M}_w = 50\,000\text{--}75\,000$), sodium dodecyl sulfate (SDS) and hexadecyltrimethylammonium bromide (HTAB) were purchased from SIGMA. All the chemicals and reagents were used as received without further purification. The PLA nanoparticles were prepared by adding dropwise 1 mL dilute solution of PLA in acetone into 100 mL water in the presence of surfactant. The surfactant concentration was kept 4 times of its corresponding critical micelle concentration (CMC). As expected, acetone quickly mixed with water as soon as it was dropped in. Therefore, insoluble hydrophobic PLA chains immediately underwent intrachain contraction and interchain association in water to form small particles. The adsorption of surfactant on the particle surface could stabilize them in water over months. The small amount of acetone (1%) introduced in the process was removed under reduced pressure, which had no effect on the size and stability of the resultant particles. The pH of the dispersion was adjusted by sodium hydroxide (NaOH) aqueous solution. In a typical degradation experiment, a proper amount of dust-free NaOH aqueous solution was directly added into 2 mL dust-free dispersion inside the light scattering cell just before the measurement. Hereafter, the PLA nanoparticles stabilized by SDS and HTAB are, respectively, denoted as PLA-SDS and PLA-HTAB.

Hyperbranched poly[phthalocyanine-co-(sebacic acid)] (PC-co-SA) ($\bar{M}_w \approx 6.45 \times 10^5 \text{ g} \cdot \text{mol}^{-1}$ and [PC]/[SA] = 0.01) was synthesized by melt polycondensation of sebacic acid and tetrahydroxyphthalocyaninatozinc(II) [ZnPc(OH)₄]. The detail of synthesis can be found elsewhere.^[25] Both PLA and PC-co-SA were soluble in tetrahydrofuran (THF). Repeating the micronization process described before, i.e., the addition of a dilute solution mixture of PLA and PC-co-SA in THF dropwise into a large amount of aqueous solution in the presence of surfactant could result in stable PLA/PC-co-SA nanoparticles. THF introduced in the process was also removed under reduced pressure.

Laser Light Scattering

A commercial LLS spectrometer (ALV/SP-125) equipped with a multi-tau digital time correlator (ALV-5000) and a solid state laser (ADLAS DPY425II, output power $\approx 400 \text{ mW}$ at $\lambda = 532 \text{ nm}$) was used. In static LLS, the angular dependence of the excess absolute time-average scattered intensity, i.e., Rayleigh ratio $R_{vv}(q)$, of a dilute dispersion led to the weight-average molar mass \bar{M}_w , the second virial coefficient A_2 and the root-mean square z -average radius $\langle R_g^2 \rangle^{1/2}$ (or simply as $\langle R_g \rangle$), where q is the scattering vector. In dynamic LLS, the Laplace inversion of a measured intensity-intensity time correlation function $G^{(2)}(t, q)$ in the self-beating mode could result in a line-width distribution $G(\Gamma)$.^[26,27] For a pure diffusive relaxation, $(\Gamma/q^2)_{q \rightarrow 0, c \rightarrow 0}$ can lead to the translational diffusion coefficient D or the hydrodynamic radius R_h by the Stokes-Einstein equation. The suspension of the PLA nanoparticles and the NaOH aqueous solution used were clarified, respectively, by 0.8 and 0.1 μm Millipore filters to remove dust. $R_{vv}(q)$ and $G^{(2)}(t, q)$ were simultaneously measured during the degradation. The detail of LLS instrumentation can be found elsewhere.^[28]

UV-Vis and Fluorescence Spectroscopy

The absorption and fluorescence emission were recorded by UV-Vis spectrophotometer (Shimadzu, UV-2100) and spectrofluorometer (Shanghai analysis factory, 970CRT), respectively. The excitation wavelength used in the fluorescence measurement was 617 nm and the exiting slit width was 5 nm. The beam path used in both the cases was 1.0 cm.

Results and Discussion

Figure 1 shows a typical Zimm plot of the PLA-SDS nanoparticles in water at 25 °C, which incorporates the angular and concentration dependence of Rayleigh ratio $R_{vv}(q)$ on a single grid. The extrapolation of $[KC/R_{vv}(q)]$ to $C \rightarrow 0$ and $q \rightarrow 0$ leads to the weight average molar mass (\bar{M}_w , particle) of the nanoparticles and the slopes of $[KC/R_{vv}(q)]_{C \rightarrow 0}$ versus q^2 and $[KC/R_{vv}(q)]_{q \rightarrow 0}$ versus C , respectively, lead to $\langle R_g \rangle$ and A_2 of the nanoparticles in water. Figure 2 shows typical hydrodynamic radius distributions of the nanoparticles measured in dynamic LLS. It reveals that both the PLA-HTAB and the PLA-SDS nanoparticles are narrowly

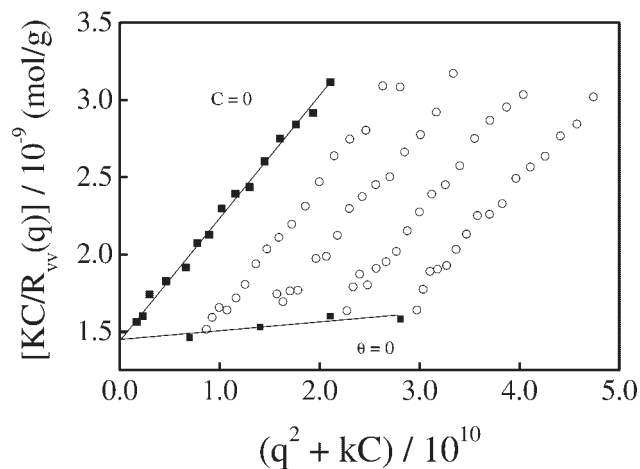


Figure 1. Typical Zimm plot of PLA-SDS nanoparticles in deionized water at $T = 25\text{ }^{\circ}\text{C}$ and $\text{pH} = 6.3$, where C ranges from 1.93×10^{-6} to $7.75 \times 10^{-6} \text{ g} \cdot \text{mL}^{-1}$.

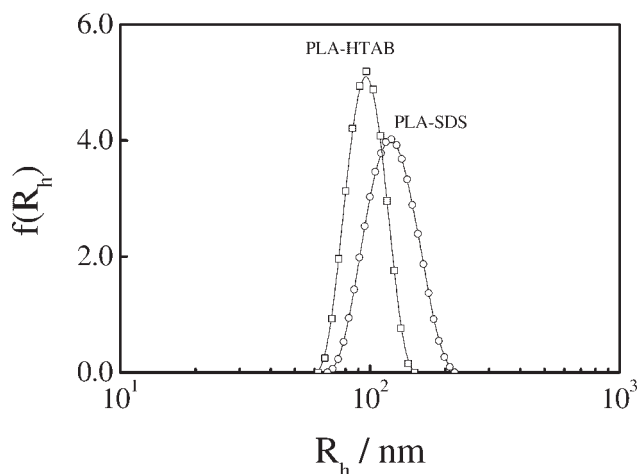


Figure 2. Typical hydrodynamic radius distributions $f(R_h)$ of PLA-SDS and PLA-HTAB nanoparticles in deionized water at $T = 25\text{ }^{\circ}\text{C}$ and $\text{pH} = 6.3$.

distributed. The average hydrodynamic radii $\langle R_h \rangle$ calculated from $\int_0^{\infty} f(R_h) R_h dR_h$ are $\approx 100 \text{ nm}$ and $\approx 120 \text{ nm}$, respectively, for the PLA-HTAB and PLA-SDS nanoparticles. It clearly shows cationic surfactant HTAB as stabilizer is more effective, which results in smaller particles.

Table 1 summarizes the LLS results of the PLA-SDS and PLA-HTAB nanoparticles in water at $\text{pH} = 6.3$, where the average aggregation number (N_{agg}) of the copolymer chains

inside each particle and the average chain density $\langle \rho \rangle$ of the particles were, respectively, estimated from $N_{\text{agg}} = \bar{M}_{w,\text{particle}} / \bar{M}_{w,\text{chain}}$ and $\langle \rho \rangle = \bar{M}_{w,\text{particle}} / (4/3\pi \langle R_h \rangle^3 N_A)$, where N_A is the Avogadro number. It is known that the ratio of $\langle R_g \rangle / \langle R_h \rangle$ reflects the conformation of a polymer chain or the density distribution of a colloid particle. For flexible coiled chains in good solvents, $\langle R_g \rangle / \langle R_h \rangle \sim 1.5$ and while for a uniform non-draining sphere, $\langle R_g \rangle / \langle R_h \rangle \approx 0.774$. The ratios of $\langle R_g \rangle / \langle R_h \rangle$ listed in Table 1 are in the range 1.0–1.1, higher than 0.774, indicating that such formed nanoparticles were partially draining, or in other words, the polymer chains inside the particles are not fully collapsed. The values of $\langle \rho \rangle$ are much lower than the chain density ($\approx 1 \text{ g} \cdot \text{cm}^{-3}$) of bulk PLA. It indicates that the polymer chains inside the nanoparticle are loosely packed with a lot of water molecules trapped inside, which is actually good for biomedical applications.^[29]

Figure 3 shows the time dependence of the relative Rayleigh ratio $[R_{v\nu}(q)]/[R_{v\nu}(q)]_0$ for PLA-SDS at $T = 37\text{ }^{\circ}\text{C}$ and $\text{pH} = 12.6$. It clearly shows that $[R_{v\nu}(q)]/[R_{v\nu}(q)]_0$ decreases as the degradation proceeds. Note that $R_{v\nu}(q) \propto NM^2$, where N and M are the number and the molar mass of the particles in the dispersion, respectively.^[30,31] The decrease of $[R_{v\nu}(q)]/[R_{v\nu}(q)]_0$ could be related to the decrease of either N or M or both. However, the inset in Figure 3 shows that there is no change in the size of the remaining PLA particles, i.e., no change in the mass of the remaining particles. Apparently, there is a contradiction because the degradation should lead to the decrease in the particle size. On the basis of the LLS theory, larger particles contribute much more to the scattered light intensity. Therefore, only those remaining PLA particles can be detected in LLS and not the small degradation products. A combination of the decrease of the scattered light intensity and the constant size of the remaining particles reveals that not all the particles were simultaneously degraded.^[9,32] The degradation is a random “one-by-one” process. The degradation of individual particles was too fast to be followed by our present LLS setup. Therefore, the decrease of $[R_{v\nu}(q)]/[R_{v\nu}(q)]_0$ in Figure 3 actually reflects a decrease in N , i.e., $[R_{v\nu}(q)]/[R_{v\nu}(q)]_0 = N/N_0 = C/C_0$ for a given volume of dispersion.

Figure 4 shows the pH dependence of the degradation at $37\text{ }^{\circ}\text{C}$. The initial slope of “ $[R_{v\nu}(q)]/[R_{v\nu}(q)]_0$ versus t ” reflects the initial degradation rate. In general, the degradation rate increases with pH. Adjusting pH, we can vary the degradation rate from minutes to days. Such a pH dependent

Table 1. Laser light-scattering characterization of poly(D,L-lactide) nanoparticles at $T = 25\text{ }^{\circ}\text{C}$ and $\text{pH} = 6.3$. The relative errors are: \bar{M}_w , $\pm 5\%$; $\langle R_g \rangle$, $\pm 8\%$; and $\langle R_h \rangle$, $\pm 2\%$.

Samples	$\bar{M}_{w,\text{particle}}$ $\text{g} \cdot \text{mol}^{-1}$	N_{agg}	A_2 $\text{mol} \cdot \text{cm}^3 \cdot \text{g}^{-2}$	$\langle R_g \rangle$ nm	$\langle R_h \rangle$ nm	$\langle R_g \rangle / \langle R_h \rangle$	$\langle \rho \rangle$ $\text{g} \cdot \text{cm}^{-3}$
SDS-PLA	7.5×10^8	1.5×10^4	5.0×10^{-5}	1.4×10^2	1.2×10^2	1.1	0.16
HTAB-PLA	2.3×10^8	4.5×10^3	1.9×10^{-4}	1.0×10^2	1.0×10^2	1.0	0.10

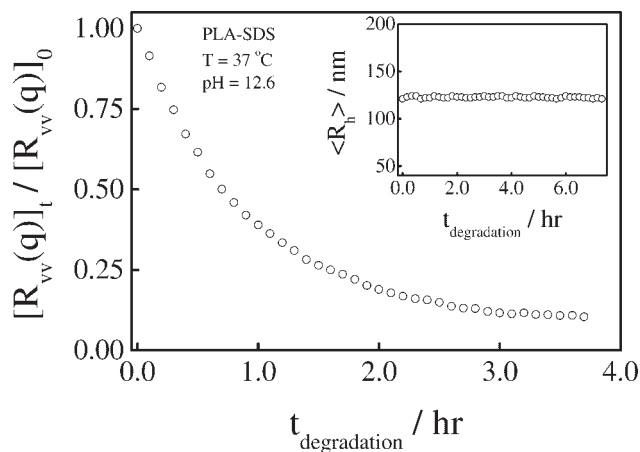


Figure 3. Kinetics of degradation of PLA-SDS nanoparticles in water, where $[R_{vv}(q)]_0$ and $[R_{vv}(q)]_t$ are the Rayleigh ratio at time 0 and t , respectively. The inset shows atypical time dependence of average hydrodynamic radius $\langle R_h \rangle$ of the remaining nanoparticles during degradation, where $C_{\text{initial}} = 3.88 \times 10^{-6} \text{ g} \cdot \text{mL}^{-1}$.

degradation is useful in the pH-regulated controllable releasing. In comparison with PLA-SDS, PLA-HTAB degraded at a relatively lower pH, or in other words, the degradation of PLA-SDS in the pH range 9–13 was much slower than PLA-HTAB. This might be due to the electrostatic repulsion between anionic SDS surfactant and OH^- , which slowed down the hydrolysis of the anhydride bond. The degradation at $\text{pH} \approx 7$ was extremely slow, which serves well for a long controllable releasing.

Figure 5 shows the temperature dependent degradation of the PLA-SDS nanoparticles at $\text{pH} = 12.6$. It is clear that the degradation rate increased with the temperature. It is helpful to note that using a higher pH is simply for the speed-up of the degradation so that the experimental time could be shortened. All the data can be well fitted by $C_t/C_0 = e^{-kt}$,

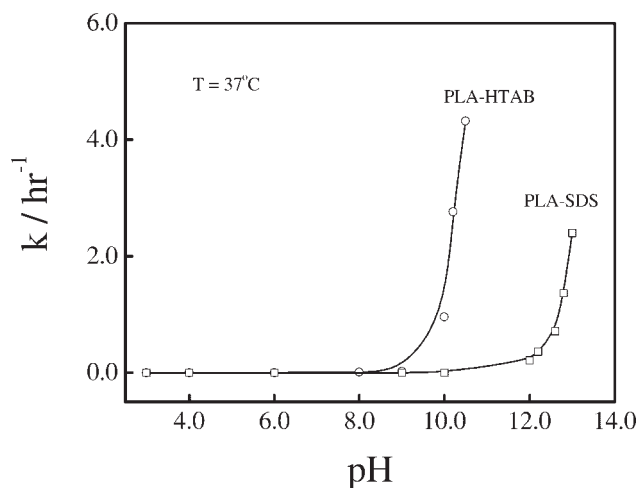


Figure 4. Comparison of degradation of PLA-HTAB and PLA-SDS nanoparticles at different pHs, where $T = 37^\circ\text{C}$ and $C_{\text{initial}} = 3.88 \times 10^{-6} \text{ g} \cdot \text{mL}^{-1}$.

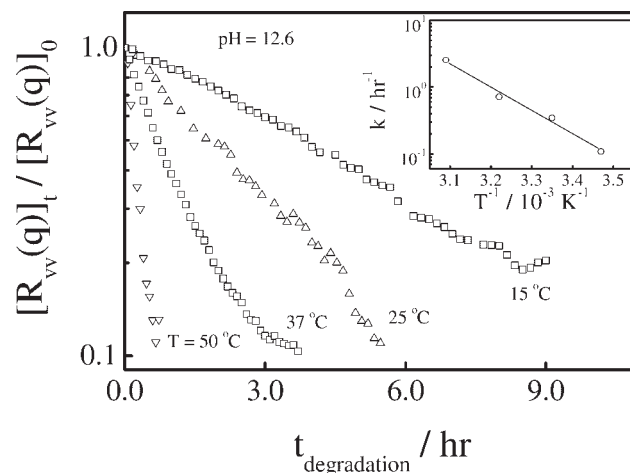


Figure 5. Temperature dependence of degradation of PLA-SDS nanoparticles, where C_0 ($3.88 \times 10^{-6} \text{ g} \cdot \text{mL}^{-1}$) and C_t are the nanoparticle concentrations at time 0 and t , respectively. The inset shows a typical Arrhenius plot of the temperature dependence of the degradation rate constant k .

indicating that the degradation followed the first-order kinetics. The least-square fitting of each curve leads to one corresponding degradation rate constant k . The inset shows a typical Arrhenius plot for the degradation, i.e., $k \propto e^{-E_a/RT}$, where the estimate of the activation energy (E_a) of the degradation is $\approx 67 \text{ kJ} \cdot \text{mol}^{-1}$. This is reasonable in comparison with the hydrolysis data in literature.^[33–35]

Our results showed that when the degradation was slow, the initial degradation rate was close to a constant; namely, the particle number degraded per unit time is constant. This is ideal for controllable releasing if we are able to entrap drugs or chemicals inside. Note that the microphase inversion used in the preparation of the PLA nanoparticles can encapsulate or entrap hydrophobic drugs into the nanoparticles. The degradation of each nanoparticle can release the drugs entrapped inside. It should be emphasized that such a controllable releasing is not based on the principle of conventional diffusion or corrosion. In conventional diffusion- or corrosion-controlled releasing, only a gradient drug concentration inside the matrix can ensure a constant releasing rate. In order to test the encapsulation and the controllable releasing, we used copolymer poly[phthalocyanine-*co*-(sebacic acid)] PC-*co*-SA, a potential chemical in photodynamic therapy (PDT). The releasing of PC-*co*-SA during the degradation was monitored by UV-vis absorption and fluorescence emission spectra.

Figure 6 and 7 reveal that the absorbance and fluorescence intensity increase as the degradation proceeds. It is known that the absorbance at 671 nm and the fluorescence at 682 nm are related the ground state of individual PC molecules.^[36] The increase in the absorbance and fluorescence intensity indicates that PC stacked inside the nanoparticles were disstacked into individual molecules after the polyester chains inside the nanoparticles were degraded into

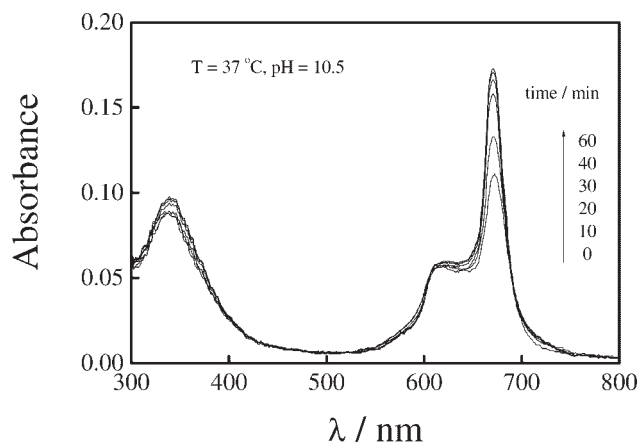


Figure 6. UV-Vis spectra of PLA-HTAB with nanoparticles encapsulated PC-co-SA ([PC-co-SA]:[PLA] = 0.2:1) during the degradation, where $C = 5.28 \times 10^{-5} \text{ g} \cdot \text{mL}^{-1}$.

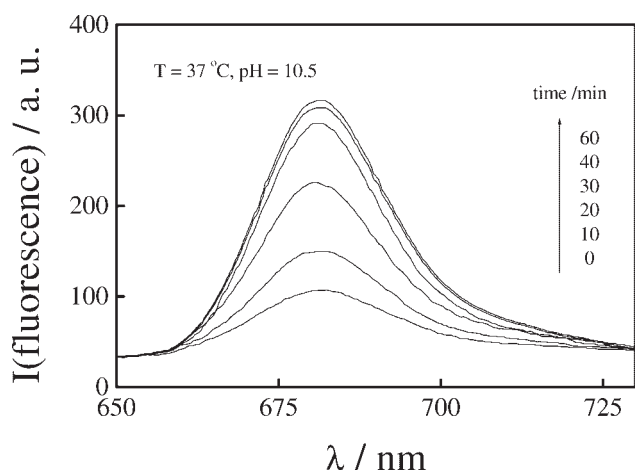


Figure 7. Fluorescence spectra of PLA-HTAB with nanoparticles encapsulated PC-co-SA ([PC-co-SA]:[PLA] = 0.2:1) during the degradation, where $C = 5.28 \times 10^{-5} \text{ g} \cdot \text{mL}^{-1}$.

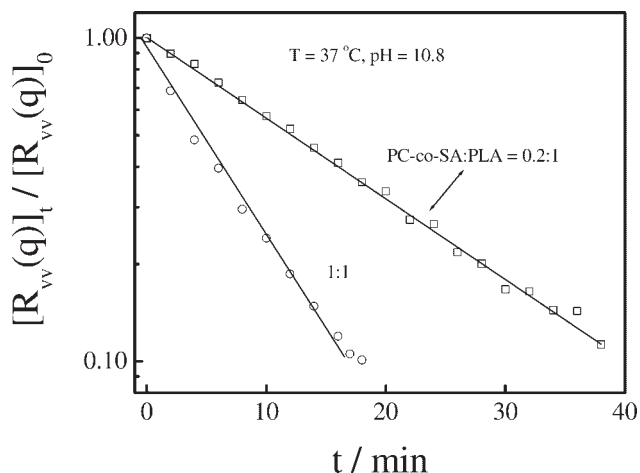


Figure 8. Degradation of PLA-HTAB nanoparticles with different amounts of encapsulated PC-co-SA [PC-co-SA]:[PLA] = 0.2:1 and 1:1, where C_0 and C_t are the nanoparticle concentrations at time 0 and t , respectively.

soluble low molar mass acids. We found that PC was released as soon as the degradation started. It was also interesting to find that the degradation rate increased with the loaded PC content, as shown in Figure 8. This provides another way to regulate the releasing rate for biomedical applications.

Conclusion

Water-insoluble poly(D,L-lactide) (PLA) can conveniently be dispersed into narrowly distributed nanoparticles stable in water via microphase inversion in the presence of surfactant. The temperature, pH and the type of surfactant used can adjust the degradation rate of such formed PLA nanoparticles. At the body temperature and $\text{pH} \approx 7$, the degradation is so slow that such a system is ideal for a long-term controllable releasing devices in biomedical applications. The degradation essentially follows the first-order kinetics. At 37°C , when $\text{pH} < 8$, the degradation practically stops, while the degradation rate increases rapidly when pH increases in the range 8–13. Therefore, such nanoparticles can entrap and protect drugs from acidic environment inside stomach so that they can be released later in basic environment inside intestine. We also determined that the activation energy of the degradation at $\text{pH} = 12.6$, calculated from a typical Arrhenius plot, is $\approx 67 \text{ kJ} \cdot \text{mol}^{-1}$.

Acknowledgements: The financial support of the CAS Bai Ren Project, the NSFC Projector (29974027) and the HKSAR Earmarked RGC Grants (CUHK4266/00P, 2160135) are gratefully acknowledged.

- [1] L. B. Peppas, *Int. J. Pharm.* **1995**, *116*, 1.
- [2] R. Lange, *Science* **1990**, *249*, 1527.
- [3] R. Langer, J. Vacanti, *Science* **1993**, *260*, 920.
- [4] R. Chandra, R. Rustgi, *Prog. Polym. Sci.* **1998**, *23*, 1273.
- [5] J. Heller, *Biomaterials* **1980**, *1*, 51.
- [6] I. Engelberg, J. Kohn, *Biomaterials* **1991**, *12*, 292.
- [7] A. C. Albertsson, S. Karlsson, *Acta Polym.* **1995**, *46*, 114.
- [8] H. Fessi, F. Puisieux, J. P. Devissaguet, S. Benita, *Int. J. Pharm.* **1989**, *55*, R1.
- [9] Z. G. Gan, T. F. Jim, M. Li, Y. Zhao, S. G. Wang, C. Wu, *Macromolecules* **1999**, *32*, 590.
- [10] M. Vert, J. Mauduit, S. Li, *Biomaterials* **1994**, *15*, 1209.
- [11] H. Shibayama, H. Yasuda, in: Y. Doi, K. Fukuda, Eds., "Biodegradable Plastics and Polymers", Elsevier, Amsterdam 1994, p. 541.
- [12] D. Lemoine, C. Francois, F. Kedzierwicz, V. Preat, M. Hoffman, P. Maincent, *Biomaterials* **1996**, *17*, 2191.
- [13] K. S. Soppimath, T. M. Aminabhavi, A. R. Kulkarni, W. E. Rudzinski, *J. Control. Rel.* **2001**, *70*, 1.
- [14] D. Duchêne, G. Ponchel, *Biomaterials* **1992**, *13*, 709.
- [15] P. Couvreur, L. Grislain, V. Lenaerts, P. Bresseur, P. Guiot, A. Biernacki, in: "Polymeric Nanoparticles and Micro-

- spheres”, P. Guiot, P. Couvreur, Eds., CRC Press, Boca Raton, FL 1986, p. 27.
- [16] D. Teshima, K. Makino, K. Mishima, Y. Itoh, R. Oishi, *Journal of Clinical Pharmacy & Therapeutics* **2002**, *27*, 79.
- [17] G. Thews, E. Mutschler, P. Vaupel, “*Anatomie, Physiologie, Pathophysiologie des Menschen*”, Wissenschaftl. Verlagsges, Stuttgart 1980, p. 229.
- [18] Z. Tuzer, P. Kratochvil, in: “*Surface and Colloid Science*”, Plenum Press, New York 1993, *15*, pp. 1–83.
- [19] B. Chu, *Langmuir* **1995**, *11*, 414.
- [20] R. Xu, M. Winnik, F. R. Hallett, G. Riess, M. D. Croucher, *Macromolecules* **1991**, *24*, 87.
- [21] T. Liu, Z. Zhou, C. Wu, B. Chu, D. K. Schneider, V. M. Nace, *J. Phys. Chem. B* **1997**, *101*, 8808.
- [22] N. Peppas, R. Langer, *Science* **1994**, *263*, 1715.
- [23] C. X. Song, V. Labhasetwar, H. Murphy, X. Qu, W. R. Humphrey, R. J. Shebuski, R. J. Levy, *J. Controlled Release* **1997**, *43*, 197.
- [24] H. K. Sah, R. Toddywala, Y. W. Chien, *J. Controlled Release* **1994**, *30*, 201.
- [25] M. G. Hu, B. Nicole, Y. Zeki, E. Johan, *J. Med. Chem.* **1998**, *41*, 1789.
- [26] B. Chu, “*Laser Light Scattering*”, 2nd edition, Academic Press, New York 1991.
- [27] B. Berne, R. Pecora, “*Dynamic Light Scattering*”, Plenum Press, New York 1976.
- [28] C. Wu, S. Q. Zhou, *Macromolecules* **1995**, *28*, 8381.
- [29] Y. Zhao, W. N. Chen, Q. Cai, S. G. Wang, J. Bo, C. Wu, *Macromolecular Bioscience* **2004**, *4*, 308.
- [30] C. Wu, K. K. Chan, *J. Polym. Sci. Polym. Phys. Ed.* **1995**, *33*, 919.
- [31] C. Wu, *J. Appl. Polym. Sci.* **1994**, *54*, 969.
- [32] Y. Zhao, T. J. Hu, Z. Lv, S. G. Wang, C. Wu, *J. Polym. Sci. Polym. Phys. Ed.* **1999**, *37*, 3288.
- [33] M. Dunne, O. I. Corrigan, Z. Ramtoola, *Biomaterials* **2000**, *21*, 1659.
- [34] C. Ladavière, T. Delair, A. Domard, C. Pichot, B. Mandrand, *Polymer Degradation and Stability* **1999**, *65*, 231.
- [35] C. Wu, J. Fu, Y. Zhao, *Macromolecules* **2000**, *33*, 9040.
- [36] T. Ngai, G. Z. Zhang, X. Y. Li, D. K. P. Ng, C. Wu, *Langmuir* **2001**, *17*, 1381.